
Article:
Luo, P., Madathil, S. orcid.org/0000-0001-6832-1300, Nishizawa, S.-I. et al. (1 more author) (2021) Turn-off dV/dt controllability in 1.2kV MOS-bipolar devices. IEEE Transactions on Power Electronics, 36 (3). pp. 3304-3311. ISSN 0885-8993

https://doi.org/10.1109/TPEL.2020.3014560

Turn-off dV/dt Controllability in 1.2kV MOS-Bipolar Devices

Peng Luo, *Student Member, IEEE*, Sankara Narayanan Ekkanath Madathil, *Senior Member, IEEE*, Shin-ichi Nishizawa, *Member, IEEE,* and Wataru Saito, *Senior Member, IEEE*

***Abstract*- Turn-off dV/dt controllability is an essential feature in IGBTs for flexible design in power switching applications. However, the occurrence of Dynamic Avalanche (DA) during the turn-off transients plays a key role on the turn-off power loss, dV/dt controllability and safe operating area of IGBTs. This paper aims to clarify the impact of DA on the turn-off characteristics of 1.2 kV trench IGBTs through 3-D TCAD simulations as well as experimental demonstrations. Measurement results show that DA is enhanced at high current density and high supply voltage conditions, which aggravates its influence on the dV/dt controllability as well as turn-off power loss. To eliminate the DA for high current density and low loss operations, a DA free design is experimentally demonstrated in the Trench Clustered IGBT (TCIGBT). Due to effective management of electric field and unique PMOS actions during turn-off, TCIGBT can retain high dV/dt controllability and low power loss at high current density operations.**

I. INTRODUCTION

Insulated Gate Bipolar Transistor (IGBT) modules are widely used as electric switches in variable power switching applications, such as Electric Vehicle (EV), industrial motor drives and transportations. In comparison to the conventional planar IGBTs, Trench-gated IGBTs (TIGBTs) with blocking voltages from 600 V up to 6.5 kV have achieved significant improvements in the switching loss (E_{off}) and on-state voltage drop ($V_{ce(sat)}$) trade-off due to higher channel density and Injection Enhancement (IE) effect [1-4]. The remarkable progress in E_{off}-$V_{ce(sat)}$ trade-off have resulted in not only higher energy efficiency but also increase in power density and cost reduction of IGBT modules. In order to increase the switching frequency of IGBT modules, high switching slopes (high dV/dt and dI/dt) are required to minimize the switching losses and delay time. However, high dV/dt can induce Electro-Magnetic Interference (EMI) noise in the electric systems due to parasitic components. Therefore, high levels of dV/dt controllability are required to meet power efficiency and EMI noise requirements in power electronic systems. Recently, it was found that high current densities and high dV/dt can induce Dynamic Avalanche (DA) during switching, which can lead to current filamentations [5-8]. The resulting excessive carriers have a significant impact on the switching slopes, power losses as well as gate stability. Since the development of TIGBTs is aimed at applications demanding ever so increasing power density, switching frequency as well as long-term reliability, the DA phenomena must be eliminated to meet these requirements. Several approaches such as deep P-float [9] and emitter gate with additional P-layer [7] have been reported to suppress but not eliminate DA in the TIGBTs. More recently, a DA free design has been experimentally demonstrated in the Trench Clustered IGBT (TCIGBT) [10]. Due to self-clamping feature and PMOS actions, the TCIGBT shows DA free performance with low power losses. Moreover, in comparison to the TIGBT, high dV/dt controllability can be maintained by TCIGBT at high operating current densities [11].

In this paper, the turn-off behavior of TIGBTs considering DA effect is explained through theoretical analysis and 3D TCAD simulations. 3D Sentaurus Device [12] within Synopsys is utilized to simulate the switching characteristics. Moreover, the turn-off transient of TCIGBT is studied in detail to explain its high dV/dt controllability. Finally, for the first time, the influence of current density and supply voltage on the turn-off dV/dt controllability of TIGBTs is investigated through experiments.

II. DV/DT LIMITATION BY DYNAMIC AVALANCHE IN TIGBTS

A. Analysis of DA in the turn-off of TIGBTs

Fig. 1 shows the simulated turn-off characteristics of a TIGBT and the circuit configuration is specified in Fig. 2. The detailed turn-off transient can be explained as follows:

Phase I: At the beginning of turn-off, the gate voltage (V_g) falls exponentially with time. The gate current (I_g) flows along the gate resistance (R_g) and discharges the gate-emitter capacitance (C_{ge}). The turn-off delay time in this phase is:

$$t_{d\_off} = R_g \times C_{ies} \times \ln\left(\frac{V_g}{V_{th} + I_c/g_m}\right) \quad (1)$$

Manuscript received April 16, 2020; revised June 22, 2020; accepted July 25, 2020.

(Corresponding author: Peng Luo)

Peng Luo and Sankara Narayanan Ekkanath Madathil are with the Department of Electronic and Electrical Engineering, University of Sheffield, Sheffield, S1 3JD, United Kingdom (e-mail: pluo2@sheffield.ac.uk; s.madathil@sheffield.ac.uk).

Shin-ichi Nishizawa and Wataru Saito are with the Research Institute for Applied Mechanics, Kyushu University, Fukuoka 816-8580, Japan (e-mail: s.nishizawa@riam.kyushu-u.ac.jp; wataru3.saito@riam.kyushu-u.ac.jp)

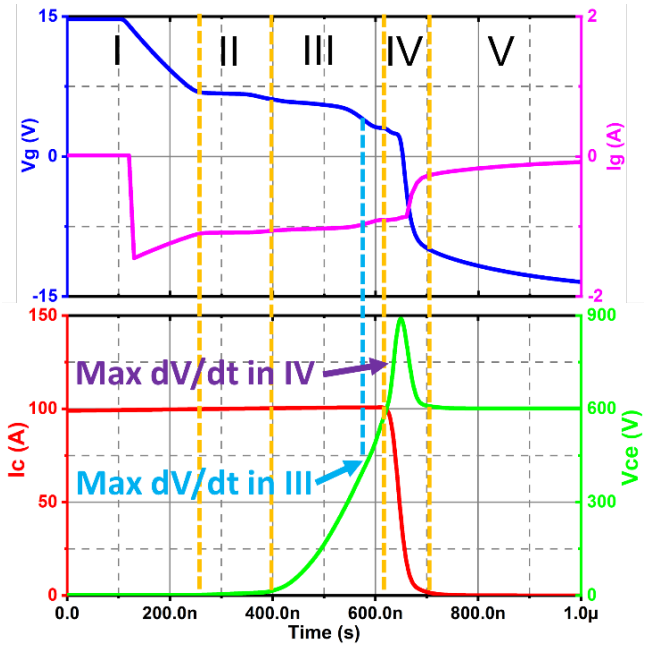

Fig. 1. Turn-off characteristics of a TIGBT. (R_g = 20 Ω)

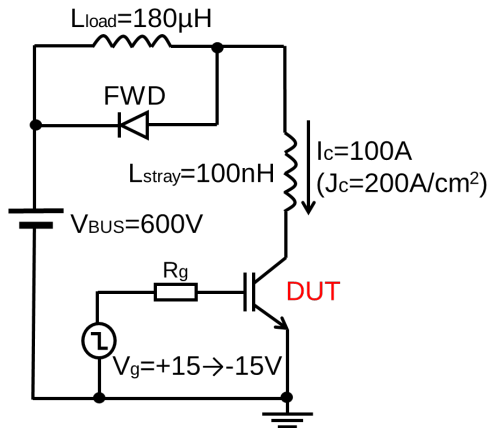

Fig. 2. Test circuit configuration.

where C_{ies} is the input capacitance, V_{th} is the threshold voltage, and g_m is the transconductance of the IGBT structure. As shown, larger R_g results in longer turn-off delay time.

Phase II: After V_g falls to the level required to maintain the collector current (I_c) at the load current level, the V_g remains constant and the I_g discharges the gate-collector capacitance (C_{gc}).

$$I_g = \frac{V_{th} + I_c/g_m}{R_g} \tag{2}$$

Phase III: The collector-emitter voltage (V_{ce}) start to rise up at a rate of

$$\frac{dV_{ce}}{dt} = \frac{I_g}{C_{GC}} = \frac{V_{th} + I_c/g_m}{R_g \times C_{GC}}. \tag{3}$$

As expressed, the dV/dt rate can be simply controlled by the

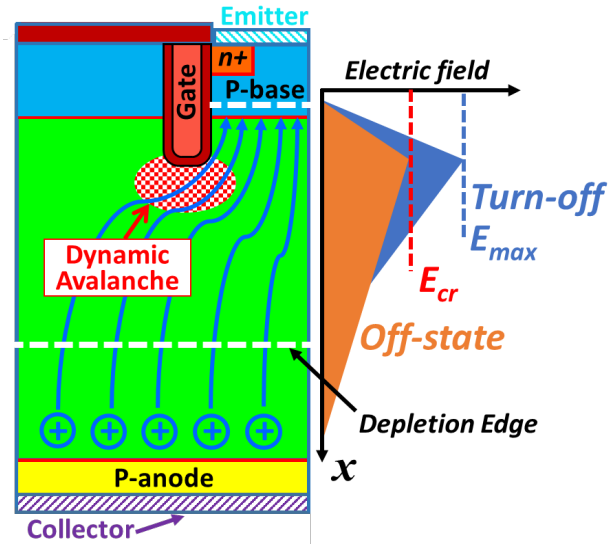

Fig. 3. Schematic of DA during turn-off of TIGBT.

R_g. The depletion region within the TIGBT expands as V_{ce} increases and the stored excessive carriers are swept out by the internal electric field. Moreover, the C_{gc} decreases due to the extension of depletion region and results in an increase in dV/dt. The maximum dV/dt appears at the point when V_g and I_g start to show a slight decrease at the end of this phase. The decrease in I_g is due to the consumption in the discharging of C_{ge} [13].

Phase IV: After V_{ce} increases to the supply voltage (V_{bus}), the Free-Wheeling Diode (FWD) turns on and the load current starts to divert from TIGBT to FWD. Therefore, the I_c decreases immediately and induces a surge voltage (V_{surge}) due to stray inductance (L_{stray}) in the circuit.

$$V_{surge} = L_{stray} \times \frac{dI_c}{dt} \tag{4}$$

If the L_{stray} is not low enough, it will result in a high dV/dt which may be even higher than that of Phase III.

Phase V: As the MOSFET structure has turned off and most of the excessive carriers have been swept out, the tail current is mainly contributed by the recombination current.

In Phases IV and V, the expanding depletion boundary is obstructed by the stored on-state carriers as depicted in Fig. 3. DA will take place if the resulting electric field (E_{max}) exceeds the critical electric field (E_{cr}), which can occur even at a voltage well below the static breakdown voltage. The detailed schematic of DA in the turn-off transient of trench gated IGBTs has been explained in [10]. The occurrence of DA results in additional excess carriers within the device, which slows down the discharging of C_{gc} (expansion of depletion region) and affects the dV/dt.

B. Influence of DA on the dV/dt Controllability

Fig. 4(a) shows the simulated turn-off waveforms of a 1.2 kV TIGBT in Field-Stop (FS) technology as a function of R_g. In practice, smaller R_g should induce larger dV/dt, as expressed in (3). However, the DA decreases the V_{surge} as well as the

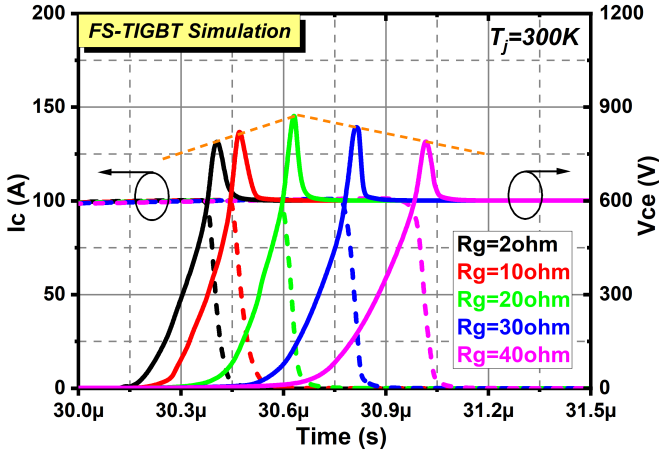

(a)

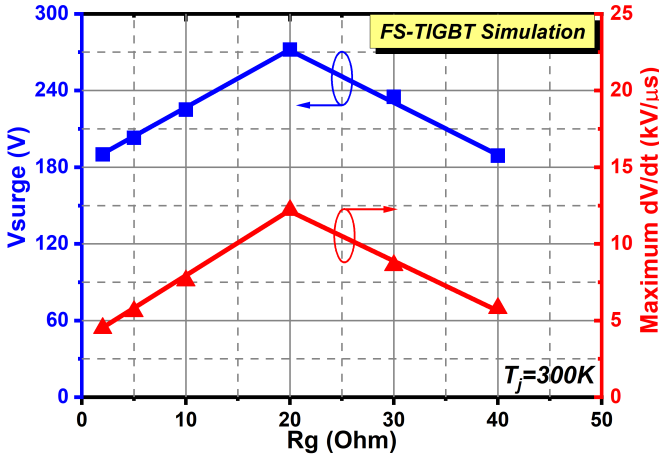

(b)

Fig. 4. Influence of R_g on (a) switch-off characteristics, and (b) surge voltage (V_{surge}) and maximum dV/dt of a conventional TIGBT, respectively.

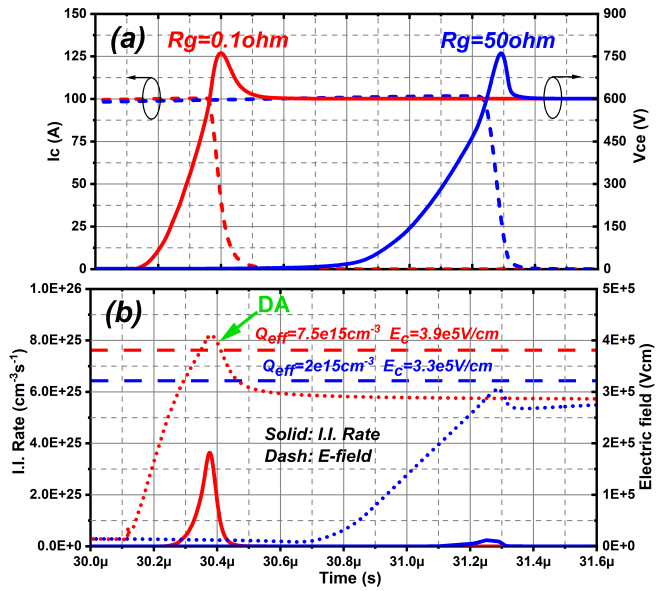

Fig. 5. Comparison of (a) Turn-off curves and (b) I.I. rates and E_{max} of a TIGBT at R_g = 0.1 Ω and R_g = 50 Ω.

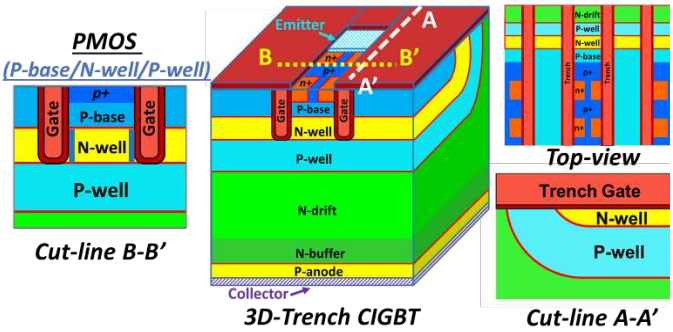

Fig. 6. 3-D cross-sectional view of TCIGBT.

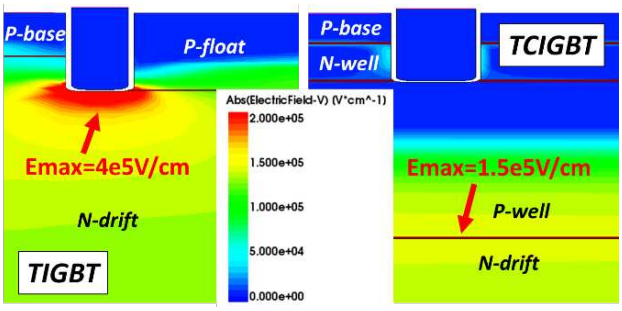

Fig. 7. Comparison of electric field distribution when V_{ce} raises to 600V during turn-off between TIGBT and TCIGBT. (R_g = 0.1 Ω).

dV/dt at small R_g conditions, as shown in Fig. 4(b). This clearly indicates that DA occurs in the cases of R_g < 20 Ω and that the dV/dt is limited by DA. The detailed reason can be explained as follows: In the cases of R_g < 20 Ω, due to faster increase in collector voltage (higher dV/dt), the stored excessive holes do not have enough time to be evacuated from the device and flow along the trench bottom, leading to a peak electric field strength which exceeds the critical value (E_c), as shown in Fig. 5(b). As a result, DA occurs and generates additional excessive charges to lower the dV/dt. Therefore, in order to meet the development of TIGBTs to satisfy various power applications, DA must be eliminated to achieve high dV/dt controllability and high switching frequency.

III. DA Free Solution – High dV/dt Controllability by TCIGBT

As a fundamental solution towards the DA elimination, TCIGBT is attractive because of its design for electric field management and unique PMOS actions [10]. Fig. 6 shows the 3D cross-sectional view of the TCIGBT. The TCIGBT device is a MOS-gated thyristor structure, which consists of P-anode, N-drift, P-well and N-well. The detailed device physics has been explained in [14]. During turn-off transient, due to the internal self-clamping feature of the TCIGBT, the N-well layer is punched through at a collector voltage of less than 20 V and the further increase in collector voltage is supported by the P-well/N-drift junction. Thus, the maximum electric field is shifted away from the trench regions. Fig. 7 compares the electric field distributions when V_{ce} increases to 600 V during

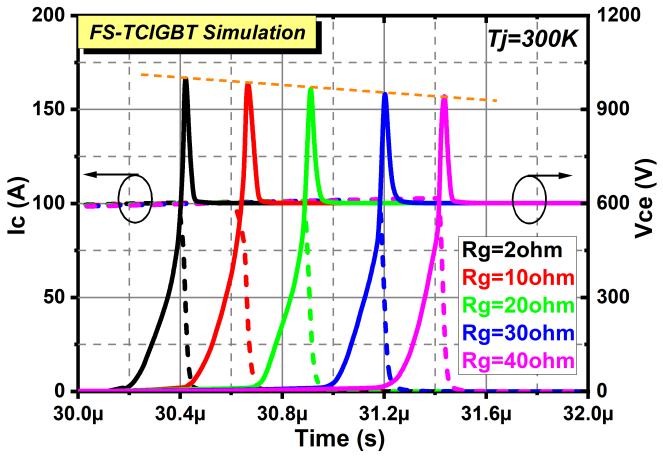

Fig. 8. Simulated switch-off waveforms of TCIGBT as a function of Rg.

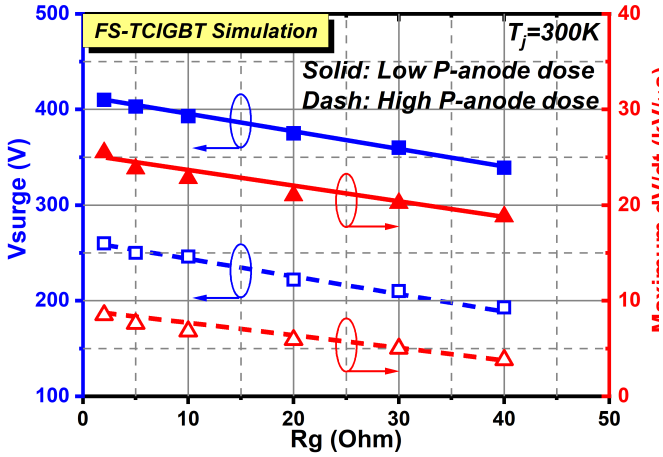

Fig. 9. V_{surge} and maximum dV/dt during turn-off of the TCIGBT.

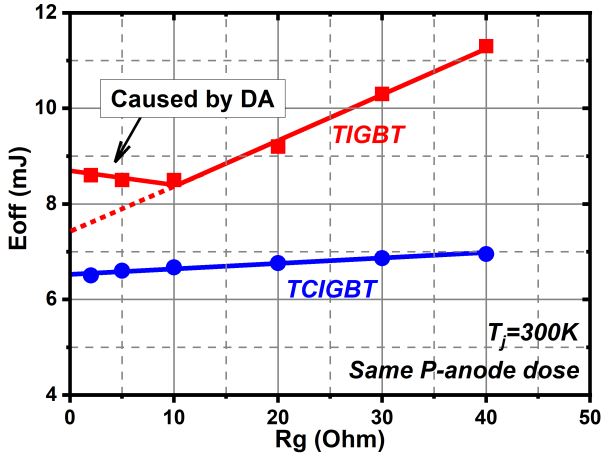

Fig. 10. Comparison of E_{off} dependence on R_g between TIGBT and TCIGBT at same P-anode dose condition.

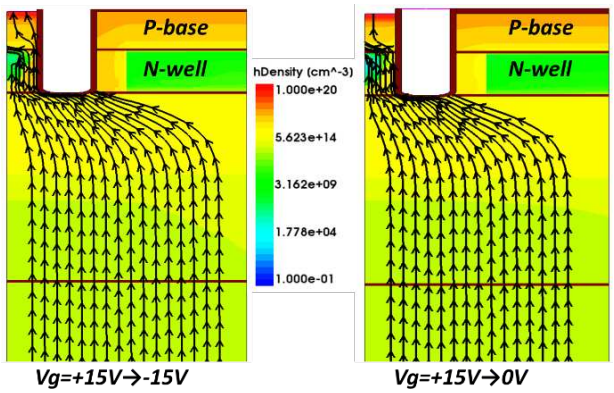

Fig. 11. Comparison of hole current flowlines at various off-state gate voltages when V_{ce} raises to 600V during turn-off of the TCIGBT.

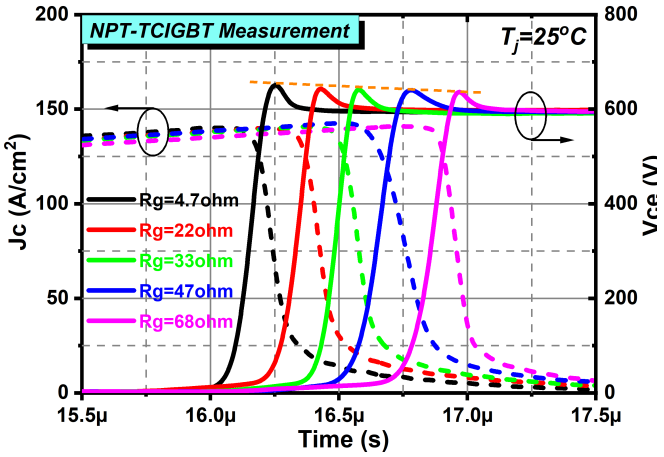

(a)

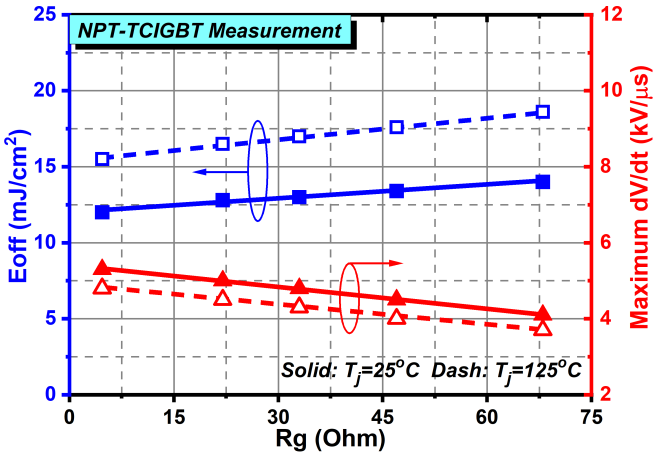

(b)

Fig. 12. Experimental results of (a) switch-off curves, (b) E_{off} and maximum dV/dt during turn-off as a function R_g of the TCIGBT.

turn-off between TIGBT and TCIGBT under R_g = 0.1 Ω and identical $V_{ce(sat)}$ (on-state carrier density) conditions. As can be seen, the trench gates of TCIGBT are protected from high electric field concentrations during turn-off. This results in effective control of the DA and dV/dt as depicted in Fig. 8 and Fig. 9. The surge voltage and dV/dt show linear increases with reduced R_g. Note that the turn-off dV/dt of TCIGBT can be easily controlled by adjusting the P-anode dose without the occurrence of DA, as shown in Fig. 9. However, in comparison, the TIGBT shows a strong electric field crowding beneath the trench bottom, which exceeds the E_{cr} and leads to a high impact ionization rate, as shown in Fig. 7. Therefore, as shown in

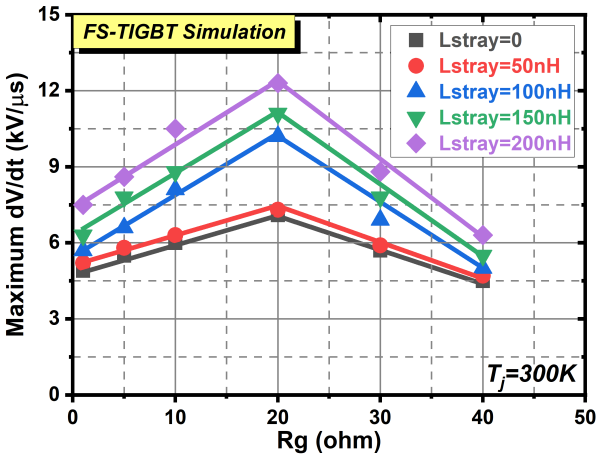

Fig. 13. Impact of stray inductance on the maximum dV/dt during turn-off of TIGBT.

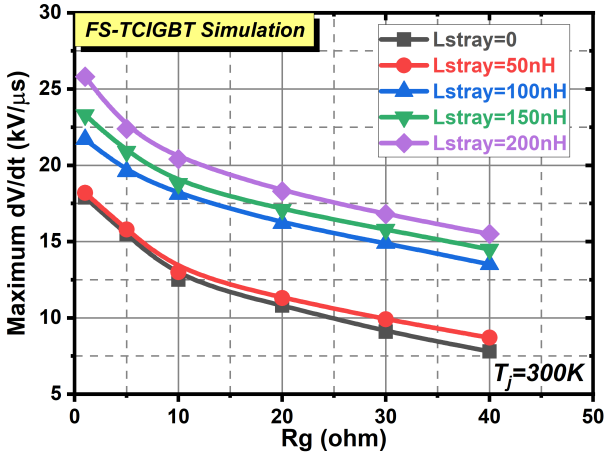

Fig. 14. Impact of stray inductance on the maximum dV/dt during turn-off of TCIGBT.

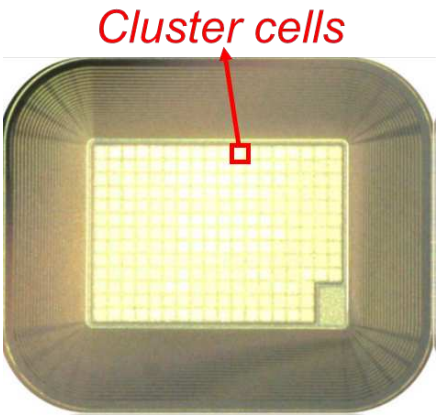

Fig. 15. Photograph of the fabricated TCIGBT device.

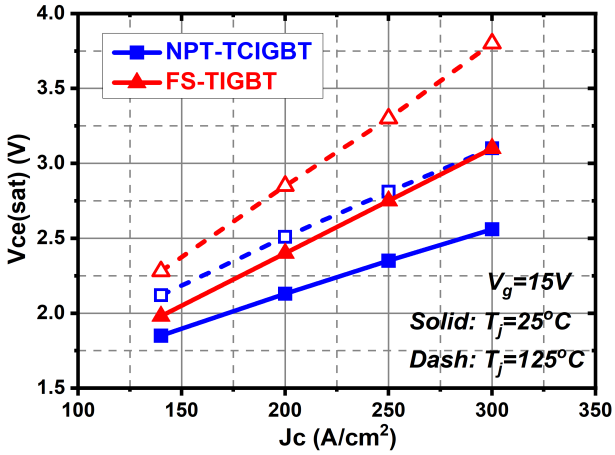

Fig. 16. Experimental results of the on-state voltage drop as a function of current density of TIGBT and TCIGBT.

Fig. 10, the TIGBT shows an increase trend of E_{off} as R_g reduces to a small value due to the occurrence of DA. However, the TCIGBT shows a linear decrease of E_{off} as R_g reduces due to DA free and the E_{off} is much lower than that of the TIGBT due to PMOS actions. The detailed reason for the reduction in E_{off} can be explained as follows: During the turn-off of TIGBT structure, hole current flows along the trench gate bottom and side wall to the P-base region [15]. As the hole current concentrates at the trench gate bottom, the hole evacuation resistance is high. In contrast, in the TCIGBT, with increase in the collector potential, the N well reaches the its self-clamping voltage, and in this process the N-well layer is fully depleted and the PMOS structure which consists of P-well, N-well and P-base is "ON". Excessive holes collected by the deep P-well are evacuated directly through the PMOS structure with low resistance by the electric field, as shown in Fig. 11. The E_{off} is therefore significantly reduced compared to that of a TIGBT, as shown in Fig. 10. In addition, note that the N-well layer is fully depleted so that the PMOS structure can turn on without the necessity of channels. Therefore, the off-state gate bias (0 V or -15 V) has no influence on the turn-off behavior of TCIGBT.

High dV/dt controllability of TCIGBT with DA free performance is confirmed from the measurement results of the turn-off waveforms and maximum dV/dt as a function of R_g of a 1.2 kV TCIGBT device [16] as shown in Figs. 12 (a) and (b), respectively. The dV/dt can be controlled even at low R_g conditions. The demonstrated devices were made in Non Punch-Through (NPT) technology. Since the DA is determined by the cathode structure design, moving from NPT technology to a thinner FS technology for improving E_{off}-$V_{ce(sat)}$ trade-off has no impact on the DA phenomenon.

IV. Impact of Stray Inductance on dV/dt Controllability

High L_{stray} can induce a high surge voltage as well as a high dV/dt during device turn-off, as expressed in Equation (4). Therefore, the L_{stray} has a significant impact on the turn-off dV/dt controllability. Fig. 13 and Fig. 14 show the simulation results of the influence of L_{stray} on the maximum dV/dt of TIGBT and TCIGBT, respectively. As shown, higher L_{stray} results in a higher maximum dV/dt in both TIGBT and TCIGBT. However, in the TIGBT, the maximum dV/dt shows decreasing trends when R_g is reduced to less than 20 Ω. This is

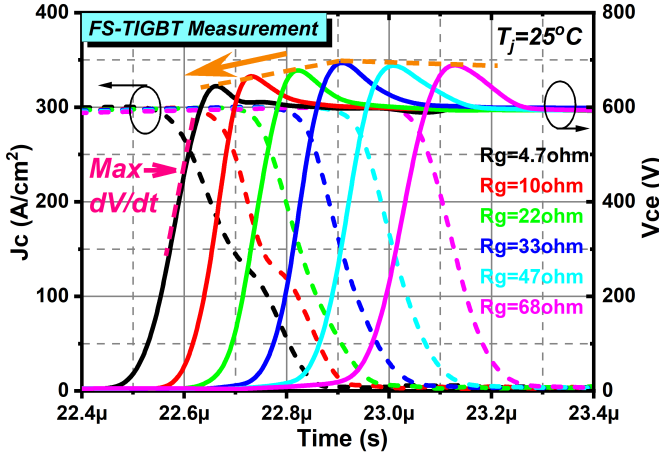

Fig. 17. Experimental results of switch-off waveforms as a function R_g of the TIGBT at J_c = 300 A/cm^2.

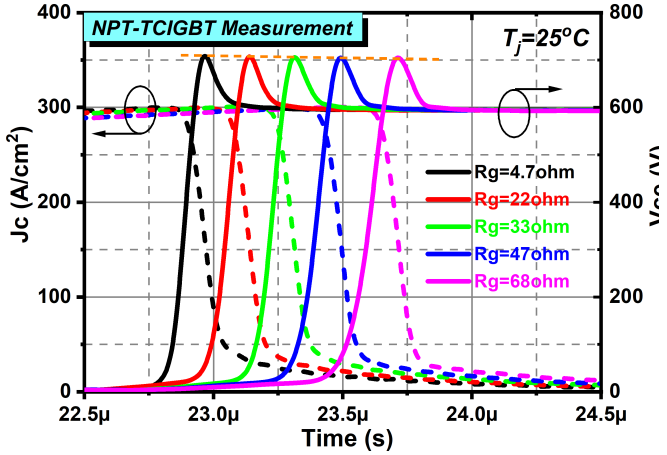

Fig. 18. Experimental results of switch-off waveforms as a function R_g of the TCIGBT at J_c = 300 A/cm^2.

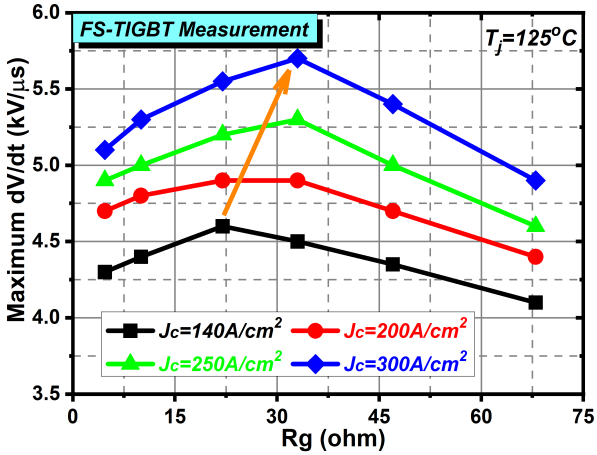

Fig. 19. Impact of current density on the maximum dV/dt during turn-off of TIGBT.

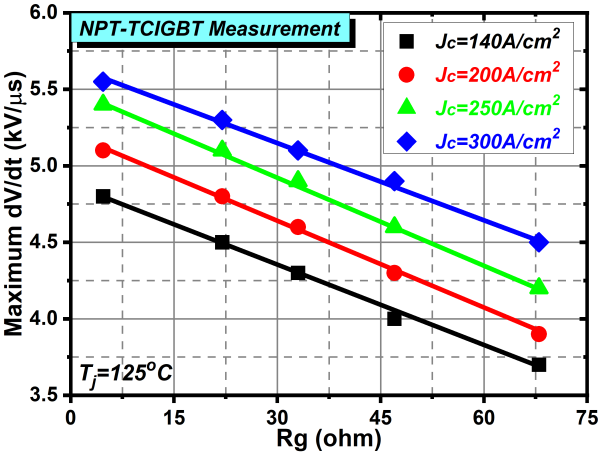

Fig. 20. Impact of current density on the maximum dV/dt during turn-off of TCIGBT.

because DA occurs at small R_g conditions, resulting in excessive charge to lower dV/dt at various L_{stray} conditions. In contrast, the dV/dt shows linear increases as R_g reduces in TCIGBT due to DA free.

V. Impact of Current Density on dV/dt Controllability

The development of IGBT modules have been devoted towards increasing power density to achieve cost reduction and flexible design for power converter systems. The requirement of higher power density is directly associated with increased operating current density with low power losses per chip area. Moreover, high dV/dt controllability at high operating current densities is also essential to satisfy various IGBT applications. In order to clarify the impact of DA on the dV/dt controllability of TIGBTs at high current densities, a 1.2 kV, 25 A TIGBT device in FS technology [17] was investigated in detail and compared with the experimental results of an NPT TCIGBT [16]. Fig. 15 shows the photograph of the fabricated 1.2 kV TCIGBT in NPT technology. The measured on-state voltage drops between the FS-TIGBT and the NPT-TCIGBT at various current densities at 25 ºC and 125 ºC are compared in Fig. 16. At both rated current density (J_c = 140 A/cm^2) and high current densities, due to thyristor conduction, the NPT TCIGBT (device thickness = 200 μm) shows much lower on-state voltage drops compared to that of FS TIGBT, which owns a much thinner device thickness of 115 μm. Fig. 17 and Fig. 18 show the turn-off waveforms as a function of R_g of TIGBT and TCIGBT at J_c = 300 A/cm^2, respectively. A decreasing trend of V_{surge} and a lower dI/dt at small R_g can be clearly observed from the case of TIGBT, which confirms the occurrence of DA. Since the surge voltage is largely independent of temperature [7], the temperature has no significant impact on the DA phenomenon. Fig. 19 and Fig. 20 show the impact of current density on the maximum dV/dt of TIGBT and TCIGBT at T_j = 125 ºC, respectively. As shown in Fig. 20, absence of DA in TCIGBT is maintained at low as well as high current densities. This is because low electric field strength beneath trench gates and high carrier evacuation speed are maintained in all conditions. Therefore, TCIGBT can maintain high dV/dt controllability even at high current densities and low power losses operations.

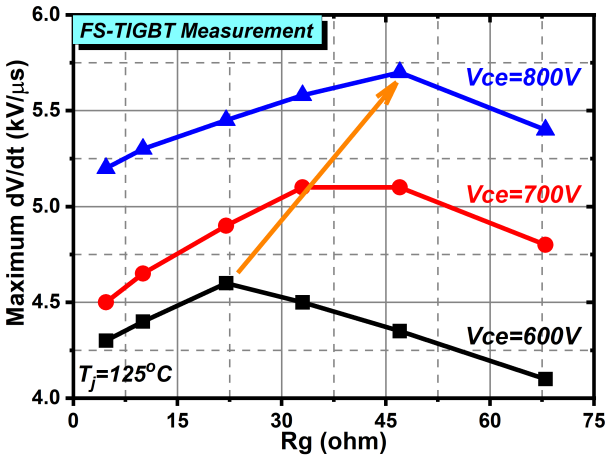

Fig. 21. Impact of supply voltage on the maximum dV/dt during turn-off of TIGBT.

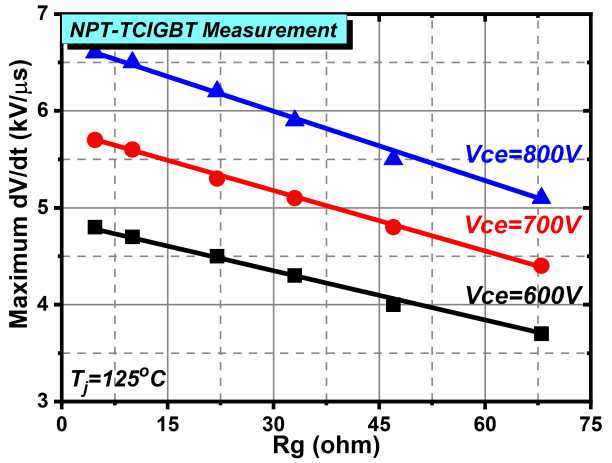

Fig. 22. Impact of supply voltage on the maximum dV/dt during turn-off of TCIGBT.

However, it is clear evident from Fig. 19 that the DA phenomenon is enhanced at high current densities in TIGBT as the peak dV/dt value appears at a larger R_g at high current densities. Note that the maximum dV/dt shows an increase with the increase of current density in both TIGBT and TCIGBT, as shown in Fig. 19 and Fig. 20. This is because high operating current densities in the experiments are achieved by increasing load currents (I_c). Therefore, the dV/dt shows increases at high current densities due to larger I_g, as expressed in Equation (3).

VI. Impact of Supply Voltage on dV/dt Controllability

As the collector voltage has a direct impact on the maximum electric field strength within the TIGBT during turn-off, the DA phenomenon is enhanced as supply voltage increases. Fig. 21 shows the measured maximum dV/dt of the TIGBT as a function of R_g at various supply voltages. As shown, the peak dV/dt value in the case of V_{ce} = 800 V appears at a larger R_g in comparison to the case of V_{ce} = 600 V, which confirms that higher supply voltage enhances the DA phenomenon of TIGBTs. In contrast, the supply voltage has no impact on the high dV/dt controllability of TCIGBT, as shown in Fig. 22.

VII. Conclusions

Detailed analysis has been undertaken to explain the impact of DA effects on the switching behavior of the 1.2 kV trench IGBT. Both simulations and experimental results confirm that DA poses fundamental limits on the reduction of switching losses as well as the dV/dt controllability of TIGBTs. In order to eliminate this phenomenon, a DA free turn-off operation is demonstrated in a TCIGBT through simulations and experiments. Absence of DA is clearly evident from the experimental results of the switching waveforms and maximum dV/dt of a TCIGBT device. Moreover, experimental results confirm that DA is enhanced at high current densities and high supply voltages, which further degrades the turn-off dV/dt controllability of TIGBTs. In contrast, TCIGBTs remain DA free performance at high current density operations and high supply voltage conditions. Therefore, as a MOS controlled thyristor device, TCIGBT can be reliably operated with very low power losses at high current densities without DA and provides high design flexibility for power electronics systems as a result of high dV/dt controllability.

References

[1] M. Harada, T. Minato, H. Takahashi, H. Nishihara, K. Inoue, and I. Takata, "600 V trench IGBT in comparison with planar IGBT-an evaluation of the limit of IGBT performance," in *Proc. 6th Int. Symp. Power Semiconductor Devices and IC's (ISPSD)*, May 1994, pp. 411-416, doi: 10.1109/ISPSD.1994.583811.

[2] T. Laska, F. Pfirsch, F. Hirler, J. Niedermeyr, C. Schaffer, and T. Schmidt, "1200 V-trench-IGBT study with square short circuit SOA," in *Proc. 10th Int. Symp. Power Semiconductor Devices and IC's (ISPSD)*, Jun. 1998, pp. 433-436, doi: 10.1109/ISPSD.1998.702738.

[3] M. Kitagawa, I. Omura, S. Hasegawa, T. Inoue, and A. Nakagawa, "A 4500 V injection enhanced insulated gate bipolar transistor (IEGT) operating in a mode similar to a thyristor," in *IEDM Tech. Dig.*, Dec. 1993, pp. 679-682, doi: 10.1109/IEDM.1993.347221.

[4] D. Werber, T. Hunger, M. Wissen, T. Schuetze, M. Lassmann, B. Stemmer, V. Komarnitskyy, and F. Pfirsch, "A 1000A 6.5kV Power Module Enabled by Reverse-Conducting Trench-IGBT-Technology," in *Proc. PCIM Europe 2015*, May 2015, pp. 1-8.

[5] T. Ogura, H. Ninomiya, K. Sugiyama, and T. Inoue, "Turn-off switching analysis considering dynamic avalanche effect for low turn-off loss high-voltage IGBTs," *IEEE Trans. Electron Devices,* vol. 51, no. 4, pp. 629-635, Apr. 2004, doi: 10.1109/TED.2004.825109.

[6] J. Lutz and R. Baburske, "Dynamic avalanche in bipolar power devices," *Microelectronics Reliability,* vol. 52, no. 3, pp. 475-481, Mar. 2012, doi: 10.1016/j.microrel.2011.10.018.

[7] S. Machida, K. Ito, and Y. Yamashita, "Approaching the limit of switching loss reduction in Si-IGBTs," in *Proc. 26th Int. Symp. Power Semiconductor Devices and IC's (ISPSD)*, Jun. 2014, pp. 107-110, doi: 10.1109/ISPSD.2014.6855987.

[8] Y. Shiba, I. Omura, and M. Tsukuda, "IGBT avalanche current filamentaion ratio: Precise simulations on mesh and structure effect," in *Proc. 28th Int. Symp. Power Semiconductor Devices and IC's (ISPSD)*, Jun. 2016, pp. 339-342, doi: 10.1109/ISPSD.2016.7520847.

[9] T. Laska, F. Hille, F. Pfirsch, R. Jereb, and M. Bassler, "Long Term Stability and Drift Phenomena of different Trench IGBT Structures under Repetitive Switching Tests," in *Proc. 19th Int. Symp. Power Semiconductor Devices and IC's (ISPSD)*, May 2007, pp. 1-4, doi: 10.1109/ISPSD.2007.4294917.

[10] P. Luo, E. M. S. Narayanan, S. Nishizawa, and W. Saito, "Dynamic Avalanche Free Design in 1.2kV Si-IGBTs for Ultra High Current Density Operation," in *IEDM Tech. Dig.*, Dec. 2019, pp. 12.3.1-12.3.4, doi: 10.1109/IEDM19573.2019.8993596.
[11] P. Luo, E. M. S. Narayanan, S. Nishizawa, and W. Saito, "High dV/dt controllability of 1.2kV Si-TCIGBT for high flexibility design with ultra-low loss operation," in *Proc. Applied Power Electronics Conference and Exposition (APEC)*, Mar. 2020.
[12] I. Synopsys, *Sentaurus Device User Guide*: Ver. L-2017. 09.
[13] Y. Onozawa, M. Otsuki, and Y. Seki, "Investigation of carrier streaming effect for the low spike fast IGBT turn-off," in *Proc. 18th Int. Symp. Power Semiconductor Devices and IC's (ISPSD)*, Jun. 2006, pp. 1-4, doi: 10.1109/ISPSD.2006.1666099.
[14] O. Spulber, M. Sweet, K. Vershinin, C. K. Ngw, L. Ngwendson, J. V. S. C. Bose, M. M. D. Souza, and E. M. S. Narayanan, "A novel trench clustered insulated gate bipolar transistor (TCIGBT)," *IEEE Electron Device Lett.,* vol. 21, no. 12, pp. 613-615, Dec. 2000, doi: 10.1109/55.887483.
[15] P. Luo, E. M. S. Narayanan, S. Nishizawa, and W. Saito, "Dynamic Avalanche Free Design in 1.2kV Si-IGBTs for Ultra High Current Density Operation," in *IEDM Tech. Dig.*, Dec. 2019, pp. 12.3.1-12.3.4, doi: 10.1109/IEDM19573.2019.8993596.
[16] H. Y. Long, M. R. Sweet, M. M. D. Souza, and E. M. S. Narayanan, "The next generation 1200V Trench Clustered IGBT technology with improved trade-off relationship," in *Proc. Applied Power Electronics Conference and Exposition (APEC)*, Mar. 2015, pp. 1266-1269, doi: 10.1109/APEC.2015.7104510.
[17] Datasheet: Available: http://pdf.tixer.ru/517408.pdf [Online].

Peng Luo (S'19) received the M.S. degree from the University of Sheffield, Sheffield, U.K., in 2015, where he is currently working toward the Ph.D. degree in the Electrical Machines and Drives Group, Department of Electronic and Electrical Engineering.
His research is focused upon the development and implementation of power semiconductor devices.

Sankara Narayanan Ekkanath Madathil (M'87, SM'00) is a Professor of Power Electronics systems in the department of Electronic and Electrical Engineering at the University of Sheffield. He works in the area of power microelectronics. He has more than three decades of proven track record in power semiconductor devices and associated technologies and works with key supply chain partners world-wide.

Shin-ichi Nishizawa (M'11) received the B.Eng., M.Eng., and Dr.Eng. in chemical engineering from Waseda University, Tokyo, Japan, in 1989, 1991, and 1994, respectively.
He then joined Waseda University as a Research Associate. In 1996, he joined the Electrotechnical Laboratory, Tsukuba, Japan (since 2001, The National Institute of Advanced Industrial Science and Technology). Since 2017, he has been with Kyushu University, Kasuga, Japan. He has worked on power semiconductor material process and power devices. He is the author or coauthor of over 150 publications and 20 patents. His research interests include semiconductor wafer technologies for power devices, power electronics components and systems.

Wataru Saito (M'04, SM'20) received the B.Eng., M.Eng., and Dr.Eng. degrees in electrical and electronics engineering from Tokyo Institute of Technology, Tokyo, Japan, in 1994, 1996, and 1999, respectively. Since 1999, he joined in Toshiba Corporation, Kawasaki, Japan, where he engaged in the development of power semiconductor devices. Since 2019, he has been with Kyushu University, Kasuga, Japan. His current interest is basic researches on the next-generation power semiconductor devices including related application technologies.